Nucl Eng Technol 47 (2015) 617–623

Available online at www.sciencedirect.com

ScienceDirect

journal homepage: http://www.journals.elsevier.com/nuclear-engineering-and-technology/

Original Article

FABRICATION OF ZrO_2-BASED NANOCOMPOSITES FOR TRANSURANIC ELEMENT-BURNING INERT MATRIX FUEL

QUSAI MISTARIHI [a], MALIK A. UMER [b], JOON HUI KIM [b], SOON HYUNG HONG [b], and HO JIN RYU [a,*]

[a] Department of Nuclear and Quantum Engineering, Korea Advanced Institute of Science and Technology, 291 Daehakro, Yuseong, Daejeon 305-701, South Korea

[b] Department of Materials Science and Engineering, Korea Advanced Institute of Science and Technology, 291 Daehakro, Yuseong, Daejeon 305-701, South Korea

ARTICLE INFO

Article history:
Received 5 January 2015
Received in revised form
13 April 2015
Accepted 8 May 2015
Available online 27 May 2015

Keywords:
Carbon fiber
Carbon foam
Graphite
Spark plasma sintering
Thermal conductivity
ZrO_2-Based composites

ABSTRACT

ZrO_2-based composites reinforced with 6.5 vol.% of carbon foam, carbon fiber, and graphite were fabricated using spark plasma sintering, and characterized using scanning electron microscopy and X-ray diffractometry. Their thermal properties were also investigated. The microstructures of the reinforced composites showed that carbon fiber fully reacted with ZrO_2, whereas carbon foam and graphite did not. The carbothermal reaction of carbon fiber had a negative effect on the thermal properties of the reinforced ZrO_2 composites because of the formation of zirconium oxycarbide. Meanwhile, the addition of carbon foam had a positive effect, increasing the thermal conductivity from 2.86 to 3.38 W m^{-1} K^{-1} at 1,100°C. These findings suggest that the homogenous distribution and chemical stability of reinforcement material affect the thermal properties of ZrO_2-based composites.

1. Introduction

Transuranic elements (TRU) including plutonium (Pu) and minor actinides (MA) are produced as a result of uranium-bearing fuel. This has resulted in a TRU stockpile. A typical nuclear power reactor generates 28 kg of Pu per Terawatt-hour (TW h) (reactor-grade Pu) [1]. In addition, the dismantling of nuclear weapons is expected to produce Pu (weapon-grade Pu). Moreover, the world stockpile of MA is estimated to be about 3 kilotons (kt) [2]. The increasing stockpile of TRU (Pu and MA) in spent fuel can be managed by burning them in fission reactors. One way of burning TRU that has been proposed is the inert matrix fuel (IMF) concept, where a U-free matrix is used to avoid additional TRU generation [3].

The concept of the IMF was developed in the early 1960s with the objective of solving the problem of Pu surplus, by burning it in light and heavy water reactors. Based on this objective, the potential matrices for IMFs are required to have a low neutron

* Corresponding author.
E-mail address: hojinryu@kaist.ac.kr (H.J. Ryu).

http://dx.doi.org/10.1016/j.net.2015.05.003
1738-5733/Copyright © 2015, Published by Elsevier Korea LLC on behalf of Korean Nuclear Society.

absorption cross section, good thermal conductivity, good chemical stability, a high melting point, and high density [3]. The performance of an IMF is very important for commercial usage. In terms of the suitability of IMF for waste disposal, the chemical stability of an IMF should make it a suitable and safe option for the geological disposal of radioactive waste [4]. The solubility tests performed on an IMF using a yttria-stabilized zirconia (YSZ) matrix showed that the IMF is three times less soluble than UO_2 fuel under reducing conditions, and about six times less under oxidizing conditions [5]. In terms of the irradiation stability, the irradiation test performed on the IMF using YSZ and calcium-stabilized zirconia (CSZ) as a matrix showed that IMF has good irradiation stability, but they experience a higher centerline temperature, more swelling, and greater fission gas release than the standard uranium oxide fuel (UO_2) [6].

Since the development of the IMF concept, several materials have been proposed to be used as an IMF for MA incineration, including zirconia (ZrO_2), YSZ, CSZ, MgO–ZrO_2, SiC, Si_3N_4, and most recently, zirconium metal [3,7]. Zirconia (ZrO_2) was proposed to be used as IMF first because of its outstanding radiation resistance, good chemical stability, and its low neutron absorption cross section. However, it has low thermal conductivity and it undergoes an allotropic change from a monoclinic to a tetragonal lattice structure. The allotropic changes can be avoided by using YSZ and CSZ, but still they have a low thermal conductivity [8]. The low thermal conductivity has a negative impact on the general performance of the material, causing high centerline temperatures, large temperature gradients and thermal stresses, high fission gas release, etc. [9]. Therefore, it is beneficial to enhance the thermal conductivity of IMF.

A variety of methods can be used to improve the thermal conductivity of zirconia. One way is the application of spinel composites using a mixture of $MgAl_2O_4$ and ZrO_2 as a matrix [10]. Another way is the use of heterogeneous matrices such as Cer–Cer (ceramic in an inert matrix) or cermet (ceramic in a metallic inert matrix) [11,12]. However, the material properties of the fuel matrix can be affected by the addition of a large volume fraction of a secondary element. Adding high thermal conductivity materials in small fractions so that they do not affect the other properties of the matrix material seems to be more effective.

The properties of the carbon materials—low thermal expansion coefficient, low atomic number, high thermal shock resistance, high melting point, and good thermal conductivity—make them a good choice as reinforcement materials [13]. Carbon foam is thermally stable and has a three-dimensional (3-D) structure [14]. The carbon fiber has outstanding mechanical and thermal properties, and it has been used as a reinforcement material for different materials including zirconia [15–18]. Graphite can also be a reinforcement material because it has a high stiffness and strength, in addition to its high thermal conductivity [19].

Regardless of the need for yttrium or calcium to stabilize the microstructure, this study investigated the effect of different reinforcement materials on the thermal properties of a zirconia matrix. YSZ and CSZ systems are expected to be more complicated, especially when a reinforcing phase is incorporated.

In this study, reticulated vitreous carbon foam, chopped carbon fiber, and graphite powder reinforced ZrO_2 were prepared using the spark plasma sintering (SPS) method. The samples were then characterized using scanning electron microscopy (SEM) and X-ray diffractometry (XRD) to examine the cross-sectional microstructures of the samples and identify the phases of the sintered samples, respectively. The effect of adding carbon fiber, vitreous carbon foam, and graphite to the thermal properties of ZrO_2 was studied, and the experimental results of the ZrO_2 composites with different reinforcement additives were analyzed and compared.

2. Experimental procedure

2.1. Materials

Graphite powder (Sigma-Aldrich, St. Louis, USA; 60% of the particles in the 10–20-μm size range [20]), reticulated vitreous carbon foam (Good Fellow, Huntingdon, UK; 2.5 mm in frame thickness) with an open porosity of 96.5% and chopped carbon fibers (T700, provided by Toray, Tokyo, Japan; 7 μm in diameter, 5 mm in average length) were used as reinforcement additives for the ZrO_2 (Sigma-Aldrich; 5 μm) matrix with a volume fraction of 6.5%. These materials were added to a graphite mold (13 mm in diameter) and sprayed with BN to prevent the powder from reacting with the mold.

2.2. Preparation of composite samples

The reinforced composites were prepared using different methods. For carbon foam reinforced ZrO_2 composites, the mold, containing carbon foam and ZrO_2 powder, was shaken manually to assure the ZrO_2 powder effectively filled the pores of the carbon foam. For carbon fiber and graphite reinforced ZrO_2 composites, carbon fibers or graphite particles and ZrO_2 powder were mixed using a ball mill machine (with a powder/ball ratio of 1:15) for 12 hours.

2.3. Sintering

The samples were sintered using SPS at a heating rate of 100°C/min and held at a temperature of 1,700°C for 10 minutes in a vacuum level of 10^{-3} Torr under a compressive pressure of 50 MPa.

2.4. Density measurement and characterization

The sintered densities of composite pellets were measured using an Archimedes principle following the ASTM B311 standard test method, and the microstructures of the samples were observed using SEM. The crystal structures of the sintered pellets were identified with XRD.

2.5. Thermal conductivity measurement

The thermal conductivities of reinforced ZrO_2 based composite pellets were determined by measuring the thermal diffusivities, specific heat capacities, and thermal expansion coefficients at room temperature, 500°C, 800°C, and 1,100°C. A laser flash instrument (LFA457) was used to measure the

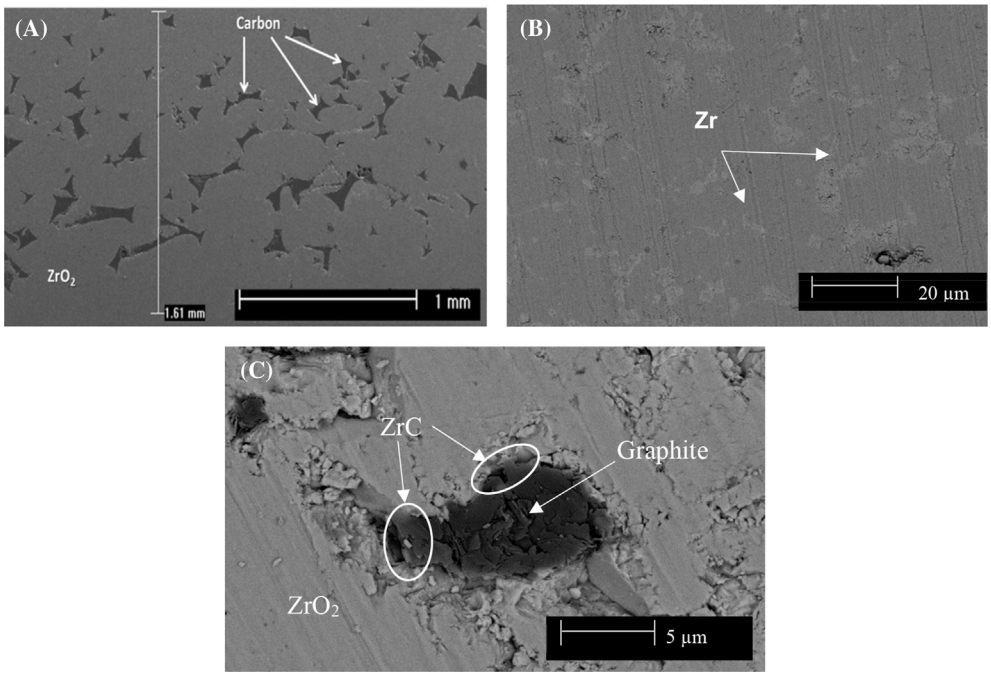

Fig. 1 – SEM images for the cross-sectional area of sintered composites. (A) Composite reinforced with carbon foam. (B) Composite reinforced with carbon fiber. (C) Composite reinforced with graphite. SEM, scanning electron microscopy.

thermal diffusivities, and differential scanning calorimetry was used to measure the specific heat capacities of composite pellets. The densities of the sintered samples at different temperatures were calculated using the thermal expansion coefficients with a measured density at 25°C.

3. Results and discussions

SEM images of the cross sections of carbon foam, carbon fiber, and graphite reinforced ZrO_2 sintered composite samples are shown in Fig. 1. For carbon foam reinforcement, the interface between the carbon foam and the ZrO_2 was identified and the structure of the carbon foam was not destroyed after sintering (Fig. 1A). This indicates that ZrO_2 effectively filled the pores of the carbon foam and prevented the collapse of the carbon foam structure. Moreover, the carbon foam was homogenously distributed in the sintered sample, creating a percolating network. For carbon fiber reinforcement, carbon fiber reacted with the ZrO_2 matrix and a new phase was detected (Fig. 1B). The graphite particles were agglomerated and randomly distributed in the sample, and an interaction layer was observed at the interface between the graphite and ZrO_2 matrix (Fig. 1C).

Fig. 2 shows the XRD analysis of carbon foam, carbon fiber, and graphite reinforced composites. As can be seen from Fig. 2, no new phase was detected in the carbon foam reinforced ZrO_2 composites and only ZrO_2 was detected (Fig. 2A), whereas both ZrC and ZrO_2 were detected in carbon fiber and graphite-reinforced ZrO_2, indicating that a reaction took place between the carbon and ZrO_2.

At a high temperature, ZrO_2 and carbon may react together through the carbothermal reduction reaction, which can result in the formation of a ZrC phase. The thermochemical properties of the constituents in the carbon containing ZrO_2 composites are shown in Table 1 [21].

Using the thermochemical properties listed in Table 1, the standard Gibbs free energy change for the carbothermal reduction reaction of ZrO_2 can be calculated using Eq. (1). Eq. (2) takes into consideration the effect of vacuum pressure (0.133 Pa) [22].

$$ZrO_{2(s)} + 3C_{(s)} \leftrightharpoons ZrC_{(s)} + CO_{(g)}$$

$$\Delta G^{\circ} = \Delta H - T\Delta S = 679,733 - 360.847\ T \tag{1}$$

$$\Delta G^{\circ} = \Delta H - T\Delta S + RT \ln\left(\frac{P_v}{P_{atm}}\right) = 679,733 - 473.426\ T, \tag{2}$$

where G° is the standard Gibbs free energy (J mol^{-1}), H is the enthalpy (J mol^{-1}), T is the temperature (K), and S is the entropy (J mol^{-1} K^{-1}). Taking thermodynamics into account, the carbothermal reduction reaction of ZrO_2 becomes more likely when the change in the Gibbs free energy becomes less than zero (i.e., 1,610°C at atmospheric pressure and 1,162.6°C at vacuum pressure in this experiment). Several studies have been published about the carbothermal reduction of zirconia with carbon materials and the main factors that affect the carbothermal reduction process [23,24]. They found that the larger the surface area and the lower the degree of graphitization, the higher the reactivity of the carbon material. Tan et al [25], Lee et al [26], and Tingry et al [27] measured the surface area of carbon foam, carbon fiber, and graphite, and by

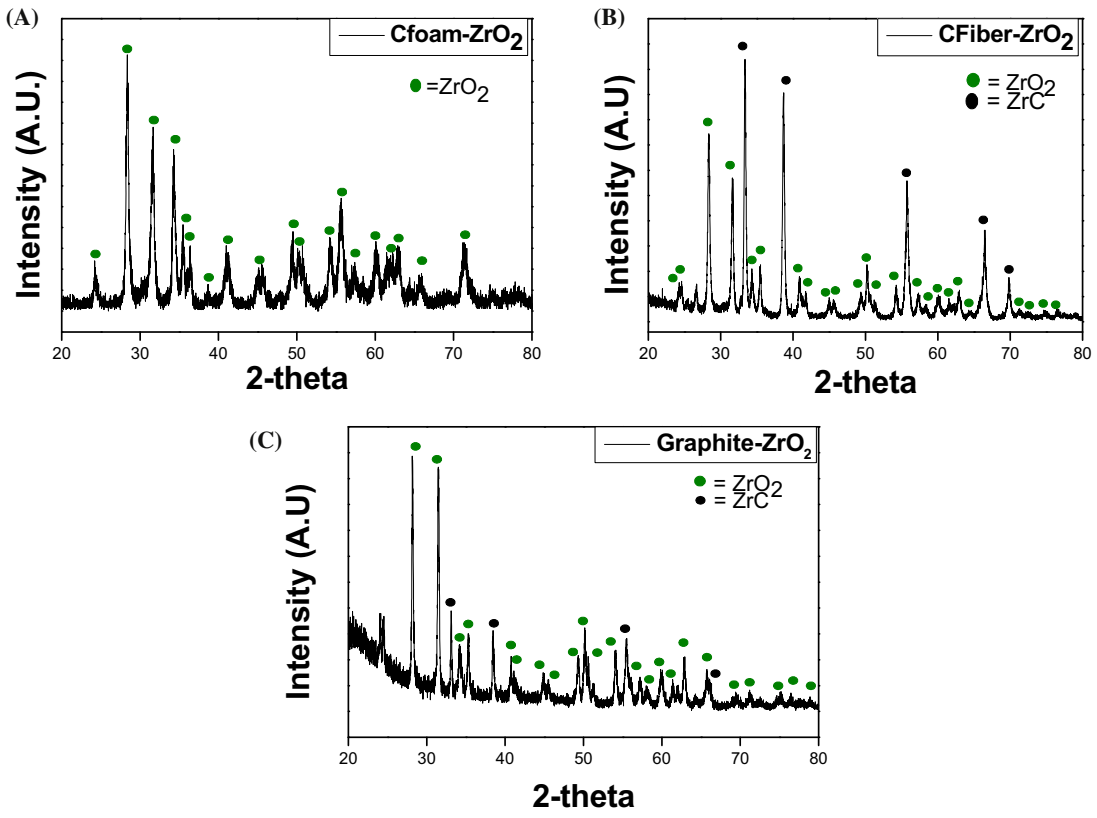

Fig. 2 – XRD analysis. (A) Carbon foam. (B) Carbon fiber. (C) Graphite-reinforced ZrO_2 composites. XRD, X-ray diffractometry.

comparing the surface area, it was found that carbon foam had the lowest value.

The thermal conductivities of pure ZrO_2 and reinforced ZrO_2 composites are shown in Fig. 3. The experimentally measured thermal conductivity values of reinforced composites were compared with the thermal conductivity values of Pure ZrO_2 at room temperature, 500°C, 800°C, and 1,100°C. The carbon foam reinforced ZrO_2 composites showed an increase in thermal conductivity, whereas the others showed a decrease in thermal conductivity compared with that of pure ZrO_2. At 1,100°C, the carbon foam reinforced ZrO_2 composites had a thermal conductivity of 3.39 W m^{-1} K^{-1}, with an increase of about 18% compared with that of pure ZrO_2. By contrast, the carbon fiber and graphite reinforced ZrO_2 composites showed relatively lower values of thermal conductivity than pure ZrO_2 composites, with a thermal conductivity of 2.06 W m^{-1} K^{-1} and 1.72 W m^{-1} K^{-1}, respectively.

Table 1 – Enthalpy and entropy for the carbothermal reduction reaction's constituents of ZrO_2.

Constituent	H (J mol^{-1}) × 10^3	S (J mol^{-1} K^{-1})
$C_{(s)}$	0	5.74
$CO_{(g)}$	−110.541	197.552
$ZrO_{2(s)}$	−1,097.463	50.358
$ZrC_{(s)}$	−196.648	33.321

The thermal conductivity of the composites depends on the thermal conductivity of the reinforcement, the porosity of the composite, and the phase formed from the chemical reaction between the composite and the reinforcements. All sintered composites were fully densified, and no pores have been observed in the sintered composites by the SEM image analysis. From the XRD and SEM analyses, it was found that

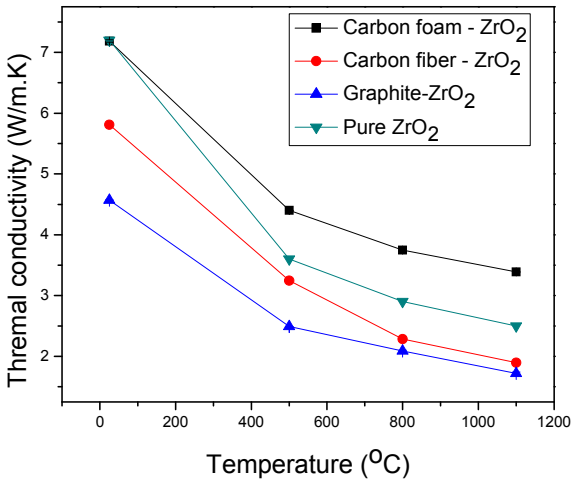

Fig. 3 – Thermal conductivity of pure ZrO_2 and reinforced ZrO_2 composites.

Table 2 – Thermal conductivity of glassy carbon and carbon foam–ZrO_2 composites measured experimentally and predicted by Maxwell–Eucken model (W m^{-1} K^{-1}) at different temperature.

Temperature (°C)	Glassy carbon [33]	Carbon foam–ZrO_2 (experimental)	Carbon foam–ZrO_2 (Maxwell–Eucken)
RT	6.96	7.18	7.47
500	9.96	4.40	4.19
800	11.27	3.75	3.58
1,100	12.36	3.39	3.16

RT, room temperature.

carbon fiber and graphite reacted with ZrO_2 through the carbothermal reduction reaction. This reaction may trigger the formation of the ZrC phase, but the thermal conductivity of ZrC is high, so this should improve the thermal conductivity of composites [28]. The carbothermal reduction reaction between zirconia and carbon was investigated by several research groups, and they reported that as a result of this reaction, a zirconium oxycarbide is formed [29]. The replacement of carbon atoms by oxygen atoms could be the reason for the low thermal conductivity of carbon fiber or graphite reinforced ZrO_2 composites. However, further investigations are necessary to confirm the formation of the oxycarbide.

Different approaches have been proposed to overcome the problem of low thermal conductivity of zirconia based on their thermal and neutronic properties, including dual-phase MgO–ZrO_2, rock-like oxide fuel ($MgAl_2O_4$–ZrO_2), and zirconia doped with erbia, yttria, and ceria [10–12]. The thermal conductivity of the rock-like fuel with 17.7% volume fraction of $MgAl_2O_4$ was measured at about 2.5 W m^{-1} K^{-1} [10]. The doped zirconia composites had a thermal conductivity of about 1.9 ± 0.15 W m^{-1} K^{-1} [11]. The dual-phase concept showed an improved thermal conductivity up to 5 W m^{-1} K^{-1}, but with a high volume fraction of 40% at 1,100°C [12]. In this study, a small volume fraction was used (up to 6.5%), and the improvement in thermal conductivity was comparable with that in previous studies where a high volume fraction of an additive phase was used. This can be attributed to the 3-D structure of carbon foam and the formation of its percolation network. The formation of the percolation network provides a path for phonons in thermal conduction and prevents phonon scattering via defects in the composites [30].

Some studies used graphene, carbon nanotubes (CNTs), and carbon fiber as reinforcement for zirconia [14,15,31,32]. Carbon fiber reinforced zirconia composites were fabricated using hot pressing at maximum temperatures of 1,400–1,650°C, and the result of that study showed that at higher sintering temperature, a new interfacial area was formed that caused the degradation of the mechanical properties of the composites [14,15]. In zirconia reinforced with CNTs at a high processing temperature, the CNTs did not retain their microstructure and underwent damage to their microstructure [31]. The graphene reinforced zirconia composites significantly increased the mechanical and electrical properties, but the thermal diffusivity increased by only 12% with the addition of graphene. This might be attributed to the small volume fraction (4.1%) [32].

The thermal conductivity for two-phase composites with low volume fraction and full densification can be calculated with adequate accuracy using the Maxwell–Eucken equation [33]

$$K = K_m \frac{(2 - 2V_r)K_m + (1 + 2V_r)K_r}{(2 + V_r)K_m + (1 - V_r)K_r},$$

where K, K_m, and K_r are the thermal conductivity for the composite, matrix, and reinforcement, respectively, and V_r is the volume fraction of the reinforcement. Zhao et al [34] proposed an empirical correlation for the thermal conductivity of glassy carbon as a function of temperature. Those values (Table 2) can be used to compare the experimental values of thermal conductivity with the values predicted by the Maxwell model for reinforced composites (Fig. 4).

As can be seen in Fig. 4, there is a good general agreement between the Maxwell model values and the measured values in terms of thermal conductivity for the carbon foam reinforced ZrO_2 composites.

4. Conclusions

Carbon foam, carbon fiber, and graphite reinforced ZrO_2-based composites were prepared using SPS at 1,700°C and characterized with SEM and XRD. The results indicate an improvement in the thermal conductivities of carbon foam

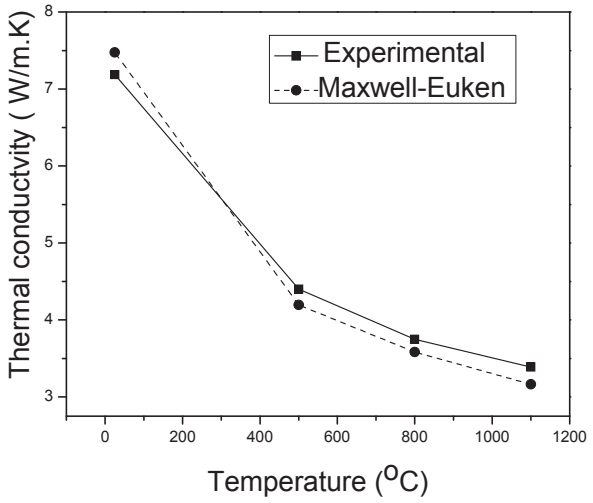

Fig. 4 – Comparison between the measured and predicted thermal conductivity values of carbon foam-reinforced ZrO_2 composites.

reinforced ZrO_2-based composites, and degradation for the carbon fiber or graphite reinforced ZrO_2-based composites.

The SEM images and XRD analyses of the reinforced composites showed that the 3-D carbon foam was homogenously distributed in the ZrO_2 matrix. In addition, no cracks were seen in the composites, and the interfaces between the reinforcement material and ZrO_2 matrix were intact. By contrast, the carbon fiber reacted with the ZrO_2 matrix completely, forming ZrC or zirconium oxycarbide. The carbothermal reduction of ZrO_2 into ZrC or zirconium oxycarbide caused degradation of the thermal properties of ZrO_2-based composites.

This study suggests that the structure and thermal stability of the reinforcement materials have major effects on the thermal conductivity of the ZrO_2-based inert matrix fuel.

Conflicts of interest

We wish to confirm that there are no known conflicts of interest associated with this publication and there has been no significant financial support for this work that could have influenced its outcome.

Acknowledgments

This study was supported by the KUSTAR–KAIST Institute, KAIST, Korea.

REFERENCES

[1] K. Hesketh, B. Lance, O. Köberl, D. Porsch, T. Wolf, G. Schlosser, H. Mineo, T. Okubo, O. Sato, S. Uchikawa, Y. Sagayama, T. Yamamoto, R. Chawla, E. Sartori, Plutonium Management in the Medium Term, NEA4451, OECD NEA, 2003.

[2] T. Yu, X. Wu, J.S. Xie, M. Qin, Z.F. Li, Z.J. Liu, H.W. Chen, A study on the burn-up characteristics of inert matrix fuels, Prog. Nucl. Energy 78 (2015) 341–345.

[3] C. Degueldre, J.M. Paratte, Concepts for an inert matrix fuel, an overview, J. Nucl. Mater. 274 (1999) 1–6.

[4] C. Lombardi, L. Luzzi, E. Padovani, F. Vettraino, Thoria and inert matrix fuels for a sustainable nuclear power, Prog. Nucl. Energy 50 (2008) 944–953.

[5] C. Degueldre, W. Wiesenack, Zirconia inert matrix fuel for plutonium and minor actinides management in reactors and as an ultimate waste form, Mater. Res. Soc. Symp. Proc. 1104 (2008) 52–62.

[6] Ch. Hellwig, M. Streit, P. Blair, T. Tverberg, F.C. Klaassen, R.P.C. Schram, F. Vettraino, T. Yamashita, Inert matrix fuel behaviour in test irradiations, J. Nucl. Mater. 352 (2006) 291–299.

[7] K. Lipkina, A. Savchenko, M. Skupov, A. Glushenkov, A. Vatulin, O. Uferov, Y. Ivanov, G. Kulakov, S. Ershov, S. Maranchak, A. Kozlov, E. Maynikov, K. Konova, Metallic inert matrix fuel concept for minor actinides incineration to achieve ultra-high burn-up, J. Nucl. Mater. 452 (2014) 378–381.

[8] C. Degueldre, T. Arima, Y.W. Lee, Thermal conductivity of zirconia based inert matrix fuel: use and abuse of the formal models for testing new experimental data, J. Nucl. Mater. 319 (2003) 6–14.

[9] K. McCoy, C. May, Enhanced thermal conductivity oxide nuclear fuels by co-sintering with BeO: II. Fuel performance and neutronics, J. Nucl. Mater. 375 (2008) 157–167.

[10] N. Nitani, T. Yamashita, T. Matsuda, S.-I. Kobayashi, T. Ohmichi, Thermophysical properties of rock-like oxide fuel with spinel–yttria stabilized zirconia system, J. Nucl. Mater. 274 (1999) 15–22.

[11] K. Idemitsu, T. Arima, Y. Inagaki, S. Torikai, M.A. Pouchon, Manufacturing of zirconia microspheres doped with erbia, yttria and ceria by internal gelation process as a part of a cermet fuel, J. Nucl. Mater. 319 (2003) 31–36.

[12] P.G. Medvedev, M.J. Lambregts, M.K. Meyer, Thermal conductivity and acid dissolution behavior of MgO–ZrO_2 ceramics for use in LWR inert matrix fuel, J. Nucl. Mater. 349 (2006) 167–177.

[13] A.A. Balandin, Thermal properties of graphene and nanostructured carbon materials, Nat. Mater. 10 (2011) 569–582.

[14] J. Klett, R. Hardy, E. Romine, C. Walls, T. Burchell, High-thermal-conductivity, mesophase-pitch-derived carbon foams: effect of precursor on structure and properties, Carbon 38 (2000) 953–973.

[15] G.H. Zhou, S.W. Wang, J.K. Guo, Z. Zhang, The preparation and mechanical properties of the unidirectional carbon fiber reinforced zirconia composite, J. Eur. Ceram. Soc. 28 (2008) 787–792.

[16] J. Ai, G. Zhou, H. Zhang, P. Liu, Z. Wang, S. Wang, Mechanical properties and microstructure of two dimensional carbon fiber reinforced zirconia composites prepared by hot-pressing, Ceram. Int. 40 (2014) 835–840.

[17] S. Guo, Thermal and electrical properties of hot pressed short pitch-based carbon fiber-reinforced ZrB_2–SiC matrix composites, Ceram. Int. 39 (2013) 5733–5740.

[18] P. He, D. Jia, T. Lin, M. Wang, Y. Zhou, Effects of high-temperature heat treatment on the mechanical properties of unidirectional carbon fiber reinforced geopolymer composites, Ceram. Int. 36 (2010) 1447–1453.

[19] S. Araby, I. Zaman, Q. Meng, N. Kawashima, A. Michelmore, H.-C. Kuan, P. Majewski, J. Ma, L. Zhang, Melt compounding with graphene to develop functional, high-performance elastomers, Nanothechnology 24 (2013) 165601–165615.

[20] M.D. Doganci, B.U. Sesli, H.Y. Erbil, B.P. Binks, I.E. Salama, Liquid marbles stabilized by graphite particles from aqueous surfactant solutions, Colloids Surf. A Physicochem. Eng. Asp. 384 (2011) 417–428.

[21] D.R. Gaskell, Introduction to the Thermodynamics of Materials, fifth ed., Taylor & Francis, New York, 2008, pp. 133–135.

[22] I. Brian, O. Knacke, Thermochemical Properties of Inorganic Substances, Springer-Verlag, Berlin, 1973, pp. 116, 162, 916, 918.

[23] M.D. Sacks, C.-A. Wang, Z. Yang, A. Jain, Carbothermal reduction synthesis of nanocrystalline zirconium carbide and hafnium carbide powders using solution-derived precursors, J. Mater. Sci. 39 (2004) 6057–6066.

[24] L.-M. Berger, P. Ettmayer, B. Schultrich, Influencing factors on the carbothermal reduction of titanium dioxide without and with simultaneous nitridation, Int. J. Refract. Met. Hard Mater. 12 (1994) 161–172.

[25] S. Tan, M. Hojeij, B. Su, G. Meriguet, N. Eugster, H.H. Girault, 3D-ITIES supported on porous reticulated vitreous carbon, J. Electroanal. Chem. 604 (2007) 65–71.

[26] Y.-J. Lee, Formation of silicon carbide on carbon fibers by carbothermal reduction of silica, Diamond Relat. Mater. 13 (2004) 383–388.

[27] S. Tingry, C. Innocent, S. Touil, A. Deratani, P. Seta, Carbon paste biosensor for phenol detection of impregnated tissue:

modification of selectivity by using β-cyclodextrin-containing PVA membrane, Mater. Sci. Eng. C 26 (2006) 222–226.
[28] S. Gomes, L. David, J.-P. Roger, G. Carlot, D. Fournier, C. Valot, M. Raynaud, Thermal conductivity degradation induced by heavy ion irradiation at room temperature in ceramic materials, Eur. Phys. J. Spec. Top 153 (2008) 87–90.
[29] M. Gendre, A. Maître, G. Trolliard, Synthesis of zirconium oxycarbide (ZrC_xO_y) powders: influence of stoichiometry on densification kinetics during spark plasma sintering and on mechanical properties, J. Eur. Ceram. Soc. 31 (2011) 2377–2385.
[30] A.N. Upadhyay, R.S. Tiwari, N. Mehta, Kedar Singh, Enhancement of electrical, thermal and mechanical properties of carbon nanotube additive $Se_{85}Te_{10}Ag_5$ glassy composites, Mater. Lett. 136 (2014) 445–448.
[31] M. Mazaheri, D. Mari, Z. Hesabi, R. Schaller, G. Fantozzi, Multi-walled carbon nanotube/nanostructured zirconia composites: outstanding mechanical properties in a wide range of temperature, Compos. Sci. Technol. 71 (2011) 939–945.
[32] Jung-Hoo Shin, Seong-Hyeon Hong, Fabrication and properties of reduced graphene oxide reinforced yttria-stabilized zirconia composite ceramics, J. Eur. Ceram. Soc. 349 (2014) 1297–1302.
[33] W.D. Kingery, Introduction to Ceramics, second ed., Wiley, New York, 1976, p. 636.
[34] B. Zhao, D. Katoshevski, E. Bar-Ziv, Temperature determination of single micrometer-sized particles from forced/free convection and photophoresis, Meas. Sci. Technol. 10 (1999) 1222–1232.